Parkos, C. A., Allen, R. A., Cochrane, C. G., & Jesaitis, A. J. (1987) *J. Clin. Invest. 80*, 732-742.
Parkos, C. A., Dinauer, M. C., Walker, L. E., Allen, R. A., Jesaitis, A. J., & Orkin, S. H. (1988) *Proc. Natl. Acad. Sci. U.S.A. 85*, 3319-3323.
Rossi, F. (1986) *Biochim. Biophys. Acta 853*, 65-89.
Rotrosen, D., Kleinberg, M. E., Nunoi, H., Leto, T. L., Gallin, J. I., & Malech, H. L. (1990) *J. Biol. Chem. 265*, 8745-8750.
Royer-Pokora, B., Kunkel, L. M., Monaco, A. P., Goff, S. C., Newburger, P. E., Baehner, R. L., Cole, F. S., Curnutte, J. T., & Orkin, S. H. (1986) *Nature 322*, 32-38.
Segal, A. W. (1989) *J. Clin. Invest. 83*, 1785-1793.
Teahan, C., Rowe, P., Parker, P., Totty, N., & Segal, A. W. (1987) *Nature 327*, 720-721.
Volpp, B. D., Nauseef, W. M., Donelson, J. E., Moser, D. R., & Clark, R. A. (1989) *Proc. Natl. Acad. Sci. U.S.A. 86*, 7195-7199.

One-Step Purification of *Actinoplanes missouriensis* D-Xylose Isomerase by High-Performance Immobilized Copper-Affinity Chromatography: Functional Analysis of Surface Histidine Residues by Site-Directed Mutagenesis†

Nadir T. Mrabet*

With the technical assistance of Ilse Van den Brande and Annemie Van den Broeck

Plant Genetic Systems, B-9000 Gent, Belgium, and Université Libre de Bruxelles, UCMB, B-1050 Brussels, Belgium
Received June 18, 1991; Revised Manuscript Received December 18, 1991

ABSTRACT: D-Xylose isomerase (XI) is a heat-stable homotetrameric enzyme used in industry for the production of high-fructose corn syrups by isomerization of D-glucose into D-fructose. To carry out biochemical and structural studies of this enzyme and of its engineered variants, a rapid and convenient method of purification of recombinant *Actinoplanes missouriensis* XI produced in *Escherichia coli* has been developed. The availability of surface-accessible histidine residues allows adsorption of XI to immobilized metal-affinity chromatography (IMAC) columns. Knowledge of the physicochemical properties of this enzyme is shown to further warrant rational modifications in the composition of the chromatographic solvents so as to achieve high selectivity in both its interaction with and its elution from a copper-loaded Chelating Sepharose Fast Flow column, an agarose-based matrix derivatized with iminodiacetic acid (IDA) groups. Purification of XI to homogeneity can thus be accomplished in a single chromatographic step starting from crude cell lysates. IDA–Cu(II)–IMAC proves convenient, fast, and reproducible. Moreover, this method is gentle to and hence suitable for mutant enzymes with decreased stability. Its disadvantage is that XI is purified in an inactive form due to inhibition by scavenged Cu^{2+}. This handicap is however easily overcome by means of a polishing step by chromatography on Mono-Q in the presence of the chelator, EDTA. Site-directed mutants have been constructed to assess the role of surface amino acid residues in the IMA recognition event. Substitution of lysine for histidine 41 results in a mutant with near wild-type properties. Yet, this mutation is shown to completely abolish adsorption to IDA–Cu(II). This finding is analyzed in relation to the structural surface properties of the XI enzyme to provide direct evidence for the implication of histidine 41 as the predominant protein ligand to IDA–Cu(II) in IMAC.

Due to rapid advances in genetic engineering, numerous proteins can now be produced efficiently in foreign host cells. Recombinant DNA technology permits replacement of any amino acid in a protein. This strategy is used in protein engineering in an effort to understand how protein structure relates to function. Such knowledge is essential to eventually design a protein with improved properties, and it requires the detailed chemical–physical and structural characterization of the wild type and of several genetically engineered variants.

The technology for purifying recombinant proteins has however lagged behind the technology for cloning the genes expressing them. When multiple variants need to be purified concurrently, it is convenient that the purification protocol be (i) simple, i.e., involves as few steps as possible; (ii) rapid, in order to avoid having to compare an "aged" reference sample with a freshly obtained mutant protein; and (iii) applicable to a large number of the protein variants being investigated.

This laboratory has been involved in the past five years in a protein engineering project aimed at improving the properties of D-xylose isomerase (XI;[1] EC 5.3.1.5) from *Actinoplanes missouriensis*. Microbial xylose isomerases are large, tet-

† This work was performed as part of a protein engineering project also supported by Gist-brocades N.V., Delft, The Netherlands, and Amylum N.V., Aalst, Belgium.

* Address correspondence to this author at the following present address: Université de Nancy I, LEGG, URA-CNRS 457, 54506 Vandœuvre-lès-Nancy, France.

[1] Abbreviations: XI, D-xylose isomerase; HPLC, high-performance liquid chromatography; IMA, immobilized metal affinity; IMAC, immobilized metal-affinity chromatography; IDA, iminodiacetic acid; IDA–Me(II) chelate complex, where Me(II) represents any divalent metal ion; IDA–Cu(II)–IMAC, IMAC with IDA–Cu(II) as affinity ligand; ASA, accessible surface area; SDH, D-sorbitol dehydrogenase; MOPS, 4-morpholinepropanesulfonic acid; EPPS, 4-(2-hydroxyethyl)-1-piperazinepropanesulfonic acid; MES, 4-morphineethanesulfonic acid; TEA, triethanolamine; Tris, Tris(hydroxymethyl)aminomethane; EDTA, ethylenediaminetetraacetic acid; kDa, kilodaltons; SDS, sodium dodecyl sulfate; PAGE, polyacrylamide gel electrophoresis.

0006-2960/92/0431-2690$03.00/0

rameric, and thermostable metalloenzymes which catalyze the isomerization of D-xylose to D-xylulose, and also that of D-glucose into the sweeter D-fructose. As a result, they have been used in industrial bioreactors at a high temperature for the manufacture of high-fructose corn syrup (HFCS). The XI gene from *A. missouriensis* has been cloned and successfully overexpressed in *E. coli* to yield a soluble, fully functional, recombinant protein.[2] The traditional purification of recombinant XI proceeds as illustrated in Figure 1. This protocol contains nine steps including sample preparation, purification, and polishing.[2] It also includes six centrifugation stages, such as those that must follow heat treatment (step III) or ammonium sulfate fractionation (step IV). Protein engineering efforts to probe structural determinants for folding, subunit assembly and interactions, stability, substrate or metal cofactor recognition, or the catalytic mechanism have generated a large number of mutants. These circumstances have naturally fostered the need for a fast purification method.

This paper describes a strategy that exploits the structural features and physicochemical properties of D-xylose isomerase from *A. missouriensis* to allow purification of this protein in a single chromatographic step using immobilized metal-affinity chromatography (IMAC), a technique that takes advantage of the property of a few amino acids to bind chelated transition metals. In IMAC, metal ions are immobilized on a hydrophilic support derivatized with a metal-chelating ligand such as iminodiacetic acid (IDA). When a protein mixture is percolated through an IMAC column, some proteins, which can bind the chelated metal through the available coordination sites, are adsorbed on the column, while others elute from the column unretarded.

Fifteen years ago, Porath (1975) postulated that amino acid residues with electron-donor character such as histidine, cysteine, and tryptophan—the "Porath's triad" (Sulkowski, 1985)—can participate in binding interactions to immobilized metal ions. This proposal has been further elegantly elaborated by Sulkowski and colleagues, who analyzed the retention behavior of several proteins in IMAC (Sulkowski, 1985, 1987, 1989; Hemdan et al., 1989). These studies attempted to rationalize phenomenological observations and correlate protein retention onto IDA–Me(II) with the availability of surface-exposed histidines. Furthermore, they suggested a significant role for the topography and the environment of histidines in modulating protein binding to IDA–Me(II). It is clear, however, that the empirical knowledge derived from the analysis of protein interactions with immobilized metal ions remained to be assessed at a molecular level. The present study further illustrates how protein structure analysis, molecular modeling, and site-directed mutagenesis can be combined to identify the amino acid ligand responsible for XI attachment to IDA–Cu(II). The participation of a specific surface histidine residue in the IMA event is directly demonstrated.

Experimental Procedures

Materials

All reagents, except where indicated otherwise, were of the highest available grade from Merck. MES was from Sigma; MOPS was from Janssen; HPLC grade, glacial acetic acid was from Burdick & Jackson; $MgCl_2$, $CoCl_2$, and $CuSO_4$ were obtained from Johnson Matthey; imidazole, 99%, was from Aldrich. EDTA and bovine serum albumin, fraction V, were from Sigma. Chelating Superose Fast Flow was from Pharmacia. All buffers were prepared using the acid forms (except for imidazole, TEA, and Tris, used as bases) in fresh Milli-Q water.

Methods

Overproduction of Recombinant Proteins. All DNA manipulations followed standard procedures (Manatis et al., 1982). Cloning of the XI gene of *A. missouriensis* (DSM43046) by complementation of the XI-deficient *Escherichia coli* strain AB1886 (Howard-Flanders et al., 1966) will be described elsewhere.[2] Wild-type and mutant enzymes were produced in soluble form in *E. coli* strain K527, a XI-negative derivative of *E. coli* K514 (Colson et al., 1965) harboring the XI-overproducing plasmid, pMa5-I, which also specifies resistance to ampicillin (Stanssens et al., 1989). Cells were grown overnight at 25 °C in a medium composed of 1% tryptone, 1% NaCl, 0.5% yeast extract, and 100 mg/mL ampicillin and centrifuged. The cell pellet was resuspended in a minimal volume of 50 mM Tris-HCl, 0.1 mM $CoCl_2$, 10 mM $MgCl_2$, 200 mM KCl, 5% glycerol, and 10 mM EDTA, pH 8.0, and lysozyme was added to a final concentration of 1 mg/mL. After standing for 20 min at 0 °C, the cells were lysed using a French press and centrifuged at 23000*g* for 30 min, and the resulting supernatant was diluted with an equal volume of 5% streptomycin sulfate. Incubation was maintained for 3 h at 4 °C and followed by centrifugation (30 min at 23000*g*). The resulting supernatant has a usual protein concentration of 18–22 mg/mL and was used as such for the purification by IDA–Cu(II)–IMAC.

Traditional Purification of Recombinant D-Xylose Isomerase and Enzymatic Assay. The traditional purification protocol of recombinant D-xylose isomerase is summarized in Figure 1 and is to be described in more detail elsewhere.[2] In brief, this protocol successively involves heating of the cell lysate supernatant after streptomycin sulfate precipitation for 30 min at 70 °C and centrifugation; ammonium sulfate fractionation of the resulting supernatant; phenyl-Superose chromatography with reverse ammonium sulfate gradient; gel permeation on Sephacryl S-200 HR; chromatography on Mono-Q with a NaCl gradient from 0 to 0.6 M; dialysis against 10 mM TEA, pH 7.2, made 10 mM EDTA (final pH is about 6); and finally dialysis against 5 mM MES, pH 6.0. It must be emphasized that purification of the metal-activated xylose isomerase in the *apoenzyme* form requires the inclusion of EDTA (10 mM) during ammonium sulfate fractionation and in *all* chromatographic solvents as indicated in Figure 1. Metal contamination was assessed by monitoring the level of residual cobalt, a metal ion which binds to XI with high affinity.[3] Metal ion determination was done by Dr. Michel Honig at the Research Institute of the Belgian Ministry of Agriculture by means of electrothermal atomic absorption spectrometry on a Varian SpectrAA 30/40 Zeeman analyzer or by sequential inductively coupled plasma-emission spectroscopy on a IL100 from Instrumentation Laboratory.

Enzyme activity was determined using the SDH (L-iditol:NAD oxidoreductase, EC 1.1.1.14) assay (Kersters-Hilderson et al., 1987), with minor modifications (Mrabet et al., 1992). One unit of enzymatic activity is the amount of enzyme required to convert 1 μmol of xylose/min under these conditions.

Protein concentrations were determined with the Bio-Rad assay (Bradford, 1976), using bovine serum albumin as a

[2] P. Stanssens et al., manuscript in preparation.

[3] J. Snauwaert, unpublished experiments. The high affinity constant, measured by equilibrium fluorescence spectroscopy, is 6.9×10^5 M^{-1}. A second cobalt binding site with a much lower affinity constant (2.2×10^3 M^{-1}) is also observed.

standard, or by absorbance at 278 nm using an absorptivity coefficient of $A_{1cm}^{0.1\%} = 1.08$.

Oligonucleotide-Directed Mutagenesis. Oligonucleotide-directed mutagenesis was done by the gapped-duplex method using the pMa/pMc phasmid vector system (Stanssens et al., 1989). Nucleotide sequence analysis made use of the dideoxy chain-termination method (Sanger et al., 1987).

IMAC Solvents Preparation. The buffers for chromatography on Cu(II)–Chelating Superose Fast Flow were prepared by a 25-fold dilution of an appropriate aliquot from a stock solution (0.5 M MMA) made up of equimolar amounts (0.5 M) of MOPS acid (pK_a 7.15 at 25 °C), MES acid (pK_a 6.09 at 25 °C), and acetic acid (pK_a 4.76 at 25 °C) and further containing 50 μM $CuSO_4$ and 5 g/L NaN_3. The presence of micromolar amounts of $CuSO_4$ in the chromatographic solvents is meant to delay the stripping of metal ions from the IMAC column caused by the presence of EDTA in cell lysates; this addition of copper ions was otherwise verified to have no influence whatsoever on the chromatographic profiles or on the properties of the eluted XI enzyme. The observation that the presence of free Cu^{2+} in micromolar amounts has no detectable effect on IMAC of other proteins and peptides has previously been documented (Figueroa et al., 1986; Hutchens & Yip, 1990). Adjustment to the desired pH was achieved by adding calculated amounts from a stock solution of 10 N NaOH. Buffer A (20 mM MMA, pH 7.0) also contained 1.0 M NaCl. Buffer B (20 mM MMA, pH 5.0) *did not contain* added salt. Buffer C (20 mM MMA) was first made 25 mM imidazole and then pH 7.0, and it *did not contain* added salt. All solvents were filter-sterilized before use through 0.2-μm Millex filters (Millipore). The MMA solvent series was inspired from the work of Figueroa et al. (1986), where, similarly, a three-component buffer mixture with equimolar amounts of HEPES, MES, and acetic acid is used to maintain the buffering capacity constant over a large pH interval and to thus ensure that the titration of buffer A with buffer B or C yields the expected continuous pH gradients. Here, MOPS was substituted for HEPES to avoid oxidative processes known to occur with piperazine ring containing "Good" buffers (Good et al., 1966) in the presence of copper ions (Hegetschweiler & Saltman, 1986; Grady et al., 1988).

Chromatographic Equipment and IMAC Procedures. All experiments were performed at room temperature. A Pharmacia HR 10/10 column was packed with 8 mL of Chelating Sepharose Fast Flow resin previously washed with Milli-Q water and suspended in an aqueous solution of 0.2 M NaCl. The column was connected to a Varian 5060 ternary-gradient HPLC system equipped with a Polychrom 9060 diode-array detector and a Spectra Physics 4290 integrator. Washing was continued at a flow rate of 2 mL/min with 50 mL of 0.2 M NaCl in H_2O, followed by 50 mL of H_2O, and finally 50 mL of buffer B (20 mM MMA, pH 5.0). The column was saturated with copper ions by injecting several aliquots of a stock solution of 10 mg/mL $CuSO_4$ in H_2O by means of a 1-mL loop mounted onto a Rheodyne automatic injector. Excess and loosely-bound metal was then removed by successive washes with a minimum of 50 mL of buffer B, 50 mL of buffer C, 50 mL of buffer B, and finally 50 mL of the appropriate equilibration buffer (see below).

At a flow rate of 1.1 mL/min, the back pressure developed by the HR 10/10 column packed with Chelating Superose Fast Flow column and mounted with a Pharmacia prefilter is only 4–6 atm. Multiple runs over several weeks could be performed reproducibly without the need for any particular maintenance: there was no indication for periodic flushing with EDTA and reloading with copper, in contrast to previous recommendations of other investigators (Figueroa et al., 1986; Hutchens et al., 1988).

To ensure reproducible results, column reequilibration between runs, however, required washing with a minimal volume of 50 mL (about 6 column volumes) of the appropriate MMA buffer mixture.

Samples prepared as described above from soluble crude *E. coli* cell lysates were injected as such onto the IMAC column in 0.5–1-mL aliquots. Since the composition of the equilibration buffer can have enormous influence on the outcome of the protein elution profile (discussed below), and due to the presence of significant amounts (~5 mM) of EDTA in the cell lysate solvent, samples larger than 5 mL were brought into the appropriate buffer conditions by extensive dialysis prior to IDA–Cu(II)–IMAC.

X-ray Structure Analysis and Molecular Modeling. A. missouriensis XI protein structure was analyzed using the 2.2-Å crystal structure of the enzyme complexed with cobalt ions and xylitol (Mrabet et al., 1992) and the BRUGEL package (Delhaise et al., 1984) on a Convex-C1 computer combined with an Evans & Sutherland PS 390 molecular graphics terminal.

Accessible surface areas (ASA) were calculated with the analytical procedure of Alard et al. (1991) using the cobalt/xylitol protein crystal structure, but after the elimination of metal ions, sugar substrates, and crystallographic water molecules. Solvent-accessible surface areas were computed using a 1.4-Å-radius solvent probe sphere (Lee & Richard, 1971). The fraction of buried residues were determined using a 5% threshold (Miller et al., 1987) on the ASA. The derived cutoff values are 12.05 Å^2 for arginine, 10.55 Å^2 for lysine, 9.7 Å^2 for histidine, 9.15 Å^2 for glutamate, and 7.55 Å^2 for aspartate [calculated from Table 2 of Miller et al. (1987)].

Sites accessible to the IDA–Cu(II) ligand were identified by means of a spherical probe with a radius of 1.93 Å. This radius size was calculated from a tridimensional model of *N*-[3-((3′-methoxy-2′-hydroxypropyl)oxy)-2-hydroxypropyl]–IDA–Cu(II) (designated below as R–IDA–Cu(II); see Figure 7) on the basis of the chemical formula given by Pharmacia in their data sheet on Chelating Sepharose Fast Flow. The structure of R–IDA–Cu(II) was built with the modeling tools present in BRUGEL using standard bond lengths, angles, and energy parameters. The IDA–ligands to the copper atom in R–IDA–Cu(II) were assumed to adopt the octahedral disposition previously described by Porath and Olin (1983) in which the nitrogen atom and the oxygen in one of the carboxylate groups (designated O21 in Figure 7A) are equatorial ligands, while the oxygen from the other carboxylate (designated O22 in Figure 7A) exists as an axial ligand. In this configuration, lines drawn from the copper atom to each of the coordination ligands are orthogonal. This starting structure was further energy-minimized by 4000 steps of steepest descent minimization (Fletcher & Reeves, 1964) using the angle constraints described above for the metal ligands while a value of 110° was imposed for the angle formed by copper, the nitrogen atom, and its adjacent carbon atom (designated C1 in Figure 7A) and a distance constraint of 2.15 Å was given to the coordination bond between copper and nitrogen. This value was chosen [see also Sundberg and Martin (1974)] as it represents the mean distance (1 SD = 0.12 Å) between copper and the coordinating nitrogen atom of histidine in selected copper proteins whose refined X-ray structures are available at high resolution. These include: azurins from *Pseudomonas aeruginosa* (1AZU), *Alcaligenes*

dentrificans (2AZA), and *Alcaligenes faecalis* (1PAZ); plastocyanin from *Populus nigra* var. italica (1PCY, 4PCY, 5PCY, and 6PCY); and bovine copper,zinc-superoxide dismutase (2SOD).

The resulting R–IDA–Cu(II) model (see Figure 7) has the following geometry. The distances from the copper atom to nitrogen, oxygens O21 and O22, and hydrogens H11 and H12 are 2.16, 1.88, 188, 3.24, and 3.03 Å, respectively. The distance between O21 and O22 is 3.16 Å, while that between H11 and H12 is 1.77 Å. The distance between the nitrogen atom and the carbon atoms C1, CA1, and CB1 is 1.51, 1.52, and 1.52 Å, respectively. Angles formed between atoms C1, N, and Cu, atoms N, Cu, and O21, atoms N, Cu, and O22, atoms O21, Cu, and O22, and atoms CA1, N, CB1 are 109.7°, 84.8°, 84.7°, 113.8°, and 111.8°, respectively. In all calculations, the van der Waals radius of the copper ion was taken as 0.87 Å (Shannon, 1976).

Results

1. Structure Analysis of A. missouriensis D-*Xylose Isomerase.* The crystal structure of *A. missouriensis* D-xylose isomerase, previously solved at 2.8-Å resolution by Rey et al. (1988), has now been further refined to 2.2 Å (Mrabet et al., 1992). The enzyme is made up of four identical subunits, each with M_r 43 330, and requires divalent metals, preferably Mg^{2+}, for enzymatic activity. Stability is also improved in the presence of metal ions such as magnesium and even more so cobalt (Mrabet et al., 1992). Each monomer is composed of an eight-stranded α/β-barrel domain followed by a C-terminal loop involved in intersubunit contacts. The active site is located deep in the middle of the α/β-barrel in close association with two distinct metal binding sites (Carrell et al., 1989; also our unpublished results).

Figure 1 describes the lengthy purification scheme traditionally used for wild-type XI. This protocol may also be used successfully with many engineered variants of xylose isomerase (our unpublished results). This finding can be rationalized on the basis of the occurrence of most of the amino acid substitutions at positions that are sequestered in the interior of the protein, and it suggests that, on the whole, the wild-type, native, protein conformation is maintained. Hence, separation methods that are surface mediated—as those listed in Figure 1—may not discriminate between wild-type and variant enzymes [for a review, see Regnier (1987)]. However, internal sites in proteins are generally sensitive to amino acid substitutions as these commonly generate mutants with reduced stability (Alber, 1987). A number of such "core" mutations, indeed, prohibit the use of the heat shock at 70 °C (see, e.g., mutant K253Q; Mrabet et al., 1992). Clearly, a more gentle purification method is needed. Furthermore, a fast purification method should help facilitate comparative analyses of variant and wild-type enzymes.

Analysis of *A. missouriensis* XI structure indicates that the molecule is highly negatively charged. In the native tetramer, surface residues are composed of 148 positively-charged amino acids (arginines + lysines) and 219 residues[4] that are negatively charged (aspartates + glutamates). Computation of solvent-accessible surface areas, based on a 5% cutoff (Miller et al., 1987), further reveals that 180 negatively-charged amino acids (Asp + Glu) against 120 positively-charged residues (Arg + Lys) can be defined as exposed to solvent. There are 10 histidine residues per subunit, most of which are buried within the protein: only 15 histidines per tetramer[4] are in contact with solvent (see Table III). Therefore, by including the charges borne by the amino- and the carboxy-termini, and by assigning a half-unit of positive charge to histidines, we can calculate that at near-neutral pH, the demetalated XI enzyme has a net charge of about −52. Even the holoenzyme, with two metal ions bound per subunit, will still bear a net negative charge of −36. Consistent with this analysis, the apoenzyme migrates on isoelectrofocusing gels to give a low p*I* between 3 and 3.5 at 10 °C (N. T. Mrabet, unpublished data).

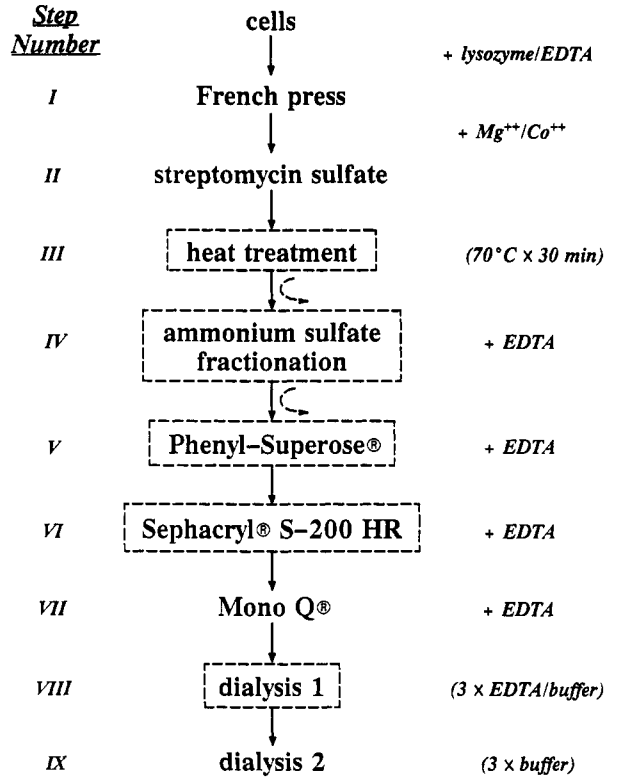

FIGURE 1: Traditional purification protocol for *A. missouriensis* D-xylose isomerase. Details are given in the Experimental Procedures section. The five purification steps replaced by a single step in the IDA–Cu(II)–IMAC procedure are boxed, while the centrifugation stages eliminated are represented by dashed curved arrows following steps III and IV.

2. Designing a Fast Purification Protocol for D-*Xylose Isomerase: Chromatography on IDA–Cu(II).* The presence of histidine residues on the surface of XI makes the enzyme a potential candidate for purification by means of IMAC (Sulkowski, 1987).

I reasoned that in a total *E. coli* cell lysate, the various components present are likely to cover a whole range of affinities for IDA–Cu(II). Consequently, elution should be performed in three successive stages: Components with low affinity would elute first, whereas those with highest affinity would be eluted last. In between, specific analytical separation of XI would be necessary.

Analytical elution of proteins bound to chelated metals has traditionally involved either a decrease of the pH of the eluent or competitive displacement with electron-donors such as imidazole. Here, I describe a strategy for protein desorption from IDA–Cu(II) which incorporates a combination of the effects of pH, ionic strength, and imidazole by means of a ternary gradient.

In the first series of experiments, the protein sample was applied onto the IDA–Cu(II)–IMAC column equilibrated in

[4] The odd number found for the surface or the solvent-accessible negatively-charged amino acids is due to deviations from symmetry larger than 1 Å in the tetramer which affect a few surface side chains. Note that this number is also dependent on the cutoff value selected to distinguish buried residues from exposed ones.

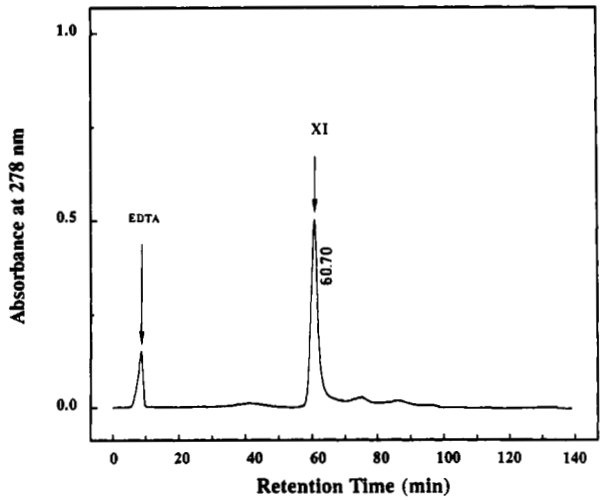

FIGURE 2: IDA–Cu(II)–IMAC of *A. missouriensis* D-xylose isomerase. The sample (0.5 mL; 5.8 mg/mL) is an aliquot of protein purified according to the protocol described in Figure 1 without further treatment. The gradient program is run as follows: (1) 99% A/1% C, isocratic for 20 min; (2) linear gradient to 99% B/1% C in 30 min, then isocratic for 10 min; (3) linear gradient to 100% C in 30 min, then isocratic for 3 min. Solvents: A = 20 mM MMA, pH 7.0, 1.0 M NaCl; B = 20 mM MMA, pH 5.0; C = 20 mM MMA, 25 mM imidazole, pH 7.0.

99% buffer A and 1% buffer C (i.e., pH 7.0, 0.99 M NaCl, 0.25 mM imidazole). Figure 2 shows that, under these conditions, XI is adsorbed onto IDA–Cu(II) as would be predicted from the presence of surface histidine residues (Sulkowski, 1987; Hemdan et al., 1990). Subsequent elution is achieved at 61 min by reducing the pH to 5 and the NaCl concentration to 0 (99% buffer B and 1% buffer C). The unretained absorbance peak with a retention time RT = 8 min does not contain protein as established by SDS–PAGE with double-staining by Coomassie and silver and is due to the presence of residual EDTA which forms a UV-absorbing complex with Cu^{2+} contained in the IMAC solvents: The presence of this chelator in XI purified by the traditional method (see Figure 1) was initially suspected from the observation of an additional absorbance peak of peculiar shape during chromatography on Mono-Q under acidic conditions (pH 5–6; Figure 3A). Authentic EDTA comigrates with this peak, yielding the same peak shape (Figure 3B). This contaminant can be eliminated by repeated centrifugal solvent exchange in 50 mM MES, pH 5–6, on Amicon PM-30 centrifugal flow cells, by treatment with high salts in slightly acidic (pH $\simeq$ 6) buffers or by dialysis against copper-containing buffers such as those used in the present study.[5] Recently, it could be shown that EDTA binds to XI with an affinity in the micromolar range.[6]

In our HPLC system, at the operating flow rate of 1.1 mL/min, the gradient lag (from the solvent gradient mixing pump to the detector flow cell) is 7 min. XI is therefore eluted at an effective retention time RT_{eff} = 54 min in the solvent gradient program given in the legend to Figure 2, i.e., in the middle of the isocratic step where pH is 5 and NaCl concentration has dropped to 0 (99% buffer B and 1% buffer C).

Figure 4A illustrates the chromatography of an aliquot of crude cell lysate prepared from *E. coli* cells expressing recombinant wild-type XI. The chromatographic profile can basically be divided into three parts. Some UV-absorbing material is eluted from the column, unretained, while other

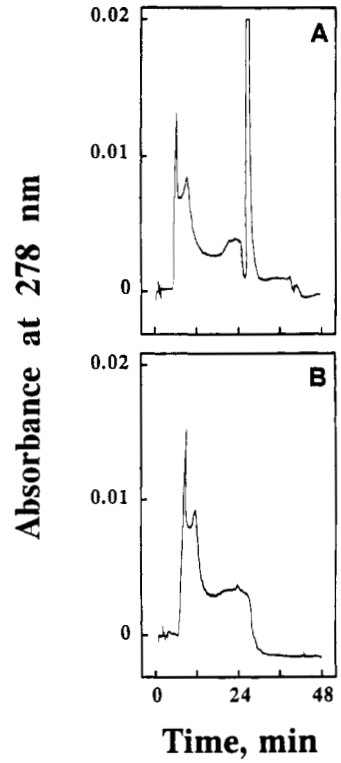

FIGURE 3: Mono-Q chromatography of D-xylose isomerase purified using the traditional method. Panel A shows the chromatographic profile of D-xylose isomerase (100 μg; $\sim$0.5 nmol) purified according to the protocol shown in Figure 1. In panel B, the protein sample has been replaced by EDTA (0.2 μmol). Solvents: A = 20 mM MES, pH 5.5; B = 20 mM MES, 0.5 M sodium acetate, pH 5.5. The gradient program is (1) 10% B, isocratic for 2 min; (2) linear gradient to 100% B in 28 min; (3) 100% B, isocratic for 5 min. The absorbance spectra recorded on line for the EDTA sample (panel B) and the first peak of panel A are identical (not shown).

components remain tightly bound when pH is reduced to 5 and further require the presence of imidazole to desorb from the IDA–Cu(II). At RT = 57 min, a peak of absorbance is observed that corresponds to the XI enzyme. The change in retention time from 61 to 57 min is very likely to result (i) from the presence of higher amounts of EDTA in crude cell lysate ($\sim$5 mM) compared to purified XI and (ii) from the competition between XI and other components in the cell lysate that display high affinity for IDA–Cu(II). SDS–PAGE analysis of the peak fractions indicates that significant purification of XI has been achieved, but it also reveals the presence of several minor contaminants (data not shown). This observation is substantiated by the examination of Figure 4A, which indeed shows significant tailing of the flow-through peak and actual overlap onto the XI peak. Since XI is eluted from IDA–Cu(II) only after the pH has reached a value of 5, this finding suggested that equilibration of the column at a lower pH, between 5 and 7, would expedite the elution of the unretained components and hence eliminate tailing, with little effect on XI itself. The pH of the equilibration buffer was consequently lowered from 7 to 6 by running the column in 50% buffer A, 49% buffer B, and 1% buffer C. This manipulation also results in lowering the initial NaCl concentration from 1 to 0.5 M. As illustrated in Figure 4B, XI still adsorbs to Cu(II)–Chelating Sepharose under these conditions, while the pH adjustment provides for a better separation of the void peak from XI. The latter is found to elute at 59 min instead of 57 min, probably because the effective (i.e., the unprotonated form) concentration of imidazole during the first 50 min of the run is decreased due to lowering the pH from

[5] N. T. Mrabet, unpublished observations.
[6] J. Snauwaert, manuscript in preparation.

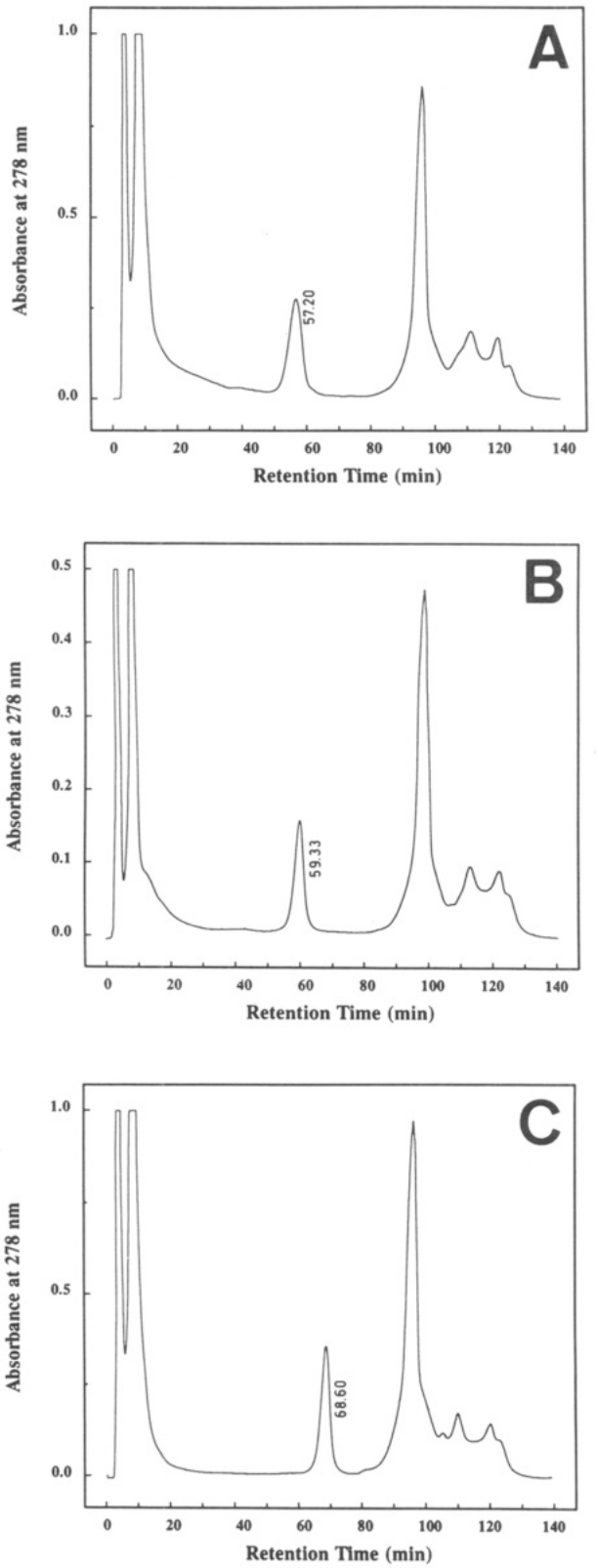

FIGURE 4: IDA–Cu(II)–IMAC of cell lysates of *E. coli* producing D-xylose isomerase. The samples (0.5 mL; ~20 mg/mL) are aliquots of the soluble supernatant obtained after streptomycin sulfate treatment of total cell lysate as described in the Experimental Procedures section. The chromatography gradient program in panel A is identical to that of Figure 2. In panel B, the gradient program is (1) 49% A/50% B/1% C, isocratic for 20 min; (2) linear gradient to 99% B/1% C in 30 min, then isocratic for 10 min; (3) linear gradient to 100% C in 30 min, then isocratic for 3 min. In panel C, the gradient program is (1) 49% A/50% B/1% C, isocratic for 20 min; (2) linear gradient to 35% A/64% B/1% C in 30 min; (3) linear gradient to 99% B/1% C in 10 min; (4) linear gradient to 100% C in 30 min, then isocratic for 3 min.

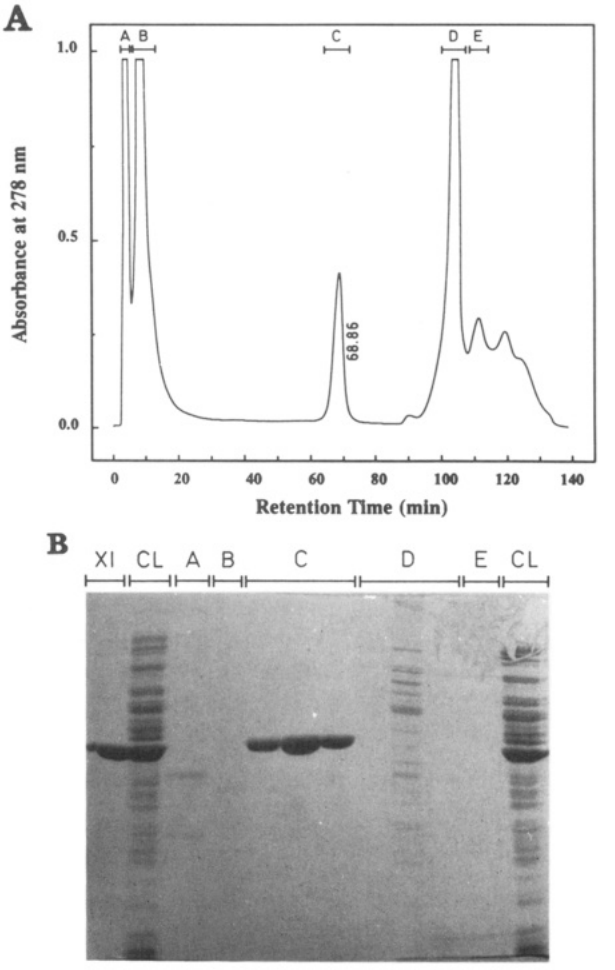

FIGURE 5: Purification by IDA–Cu(II)–IMAC of recombinant *A. missouriensis* D-xylose isomerase produced in *E. coli*. In panel A, the gradient program used is (1) 49% A/50% B/1% C, isocratic for 20 min; (2) linear gradient to 35% A/64% B/1% C in 30 min; (3) linear gradient to 99% B/1% C in 10 min; (4) linear gradient to 95% B/5% C in 15 min; (5) linear gradient to 100% C in 15 min, then isocratic for 3 min. Panel B represents an SDS–PAGE (10%) with Coomassie staining analyzing the peak fractions—labeled as in panel A—of the chromatogram; fractions were collected using a Pharmacia FRAC-200 fraction collector in the peak collection mode with a 3% cutoff; maximum fraction size was 2.2 mL. XI designates standard enzyme purified according to the protocol of Figure 1. CL is the total cell lysate supernatant after streptomycin sulfate treatment.

7 to 6. Figure 4C shows that the resolution of XI from the flow-through can be further improved by raising the pH from 5.0 to 5.7 at 50 min in the gradient program—i.e., at 57 min on the chromatogram—as the retention time of the enzyme now increases to 69 min, thereby resolving these two peaks completely. Not unexpectedly, this 10-min delay in elution also causes overlap of the XI peak with the late components. It is shown in Figure 5A that making the imidazole gradient more shallow from 60 to 75 min—i.e., 67 to 82 min on the chromatogram—allows these components to resolve away from the enzyme and to achieve baseline resolution. Figure 5B represents an SDS–PAGE analyzing the peak fractions of the chromatogram shown in Figure 5A: Purification of XI to homogeneity has clearly been achieved in a single chromatographic step.

3. Elimination of Copper Ions from D-Xylose Isomerase Purified by IDA–Cu(II)–IMAC. XI purified by IDA–Cu(II)–IMAC is contaminated with copper ions. Such contamination is readily apparent because it leads to significant enzyme inhibition. This loss of enzyme activity is observed whether or not the MMA solvents are supplemented with

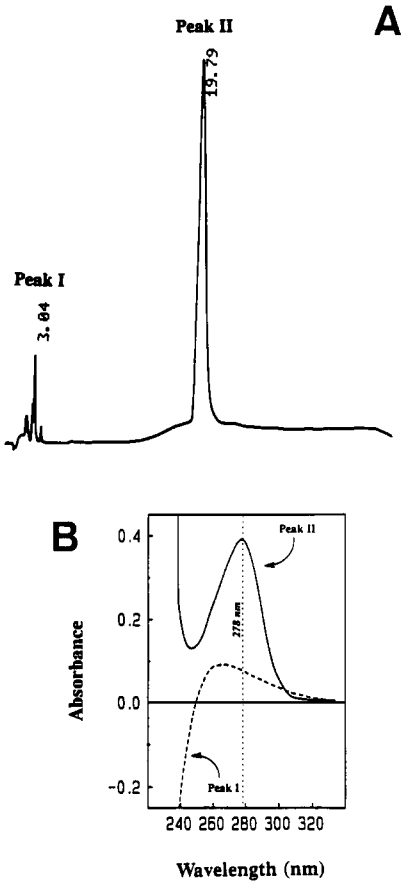

FIGURE 6: Mono-Q of D-xylose isomerase purified by IDA–Cu(II)–IMAC. Panel A shows the chromatography on Mono-Q of an aliquot (1 mL) of enzyme preparation directly obtained by IDA–Cu(II)–IMAC. The gradient program is (1) 20 mM MES, 10 mM EDTA, 0.02% NaN_3, 100 mM NaCl, pH 6.0, isocratic for 10 min; (2) linear gradient to 500 mM NaCl in 30 min. Flow rate is 2 mL/min. Panel B shows the absorbance spectra corresponding to peaks I and II of panel A.

micromolar amounts of Cu^{2+}, a finding that implies bleeding of the metal from the column, also observed by other investigators (Belew et al., 1987).

Copper ions must therefore be eliminated from the enzyme preparation. To achieve demetalation of *A. missouriensis* XI, however, turns out not to be trivial. Extensive dialysis against EDTA is not effective in fully removing high-affinity cations such as Co^{2+} or Cu^{2+}. This observation has been shared by Kasumi and colleagues for the D-xylose isomerase from *Streptomyces griseofuscus* S-41 (Kasumi et al., 1982). Inclusion of EDTA (10 mM) during ammonium sulfate fractionation and in the chromatographic solvents as indicated in Figure 1 is a powerful and *obligatory* means for eliminating metals from XI: Under these conditions, residual cobalt is found not to exceed 0.5×10^{-3} atom/$mol_{tetramer}$, while the absence of EDTA in those solvents can lead to amounts as high as 0.3 atom/mol. The affinity of divalent metal cations for XI is also reduced significantly at acidic pH (unpublished observations). These concepts were put into practice to efficiently demetalate XI as follows. After IDA–Cu(II)–IMAC, the enzyme-containing fractions were pooled and directly loaded onto a Mono-Q anion-exchange column equilibrated in 20 mM MES, 10 mM EDTA, 0.02% NaN_3, 0.1 M NaCl, pH 6.0. The Mono-Q was then washed with 20 mL of the same buffer, and the bound XI was subsequently eluted by raising the NaCl concentration to 0.5 M as shown in Figure 6A. Two absorbance peaks are evident on the chromatographic profile, one of which elutes in the void while the other

Table I: Purification of D-Xylose Isomerase[a]

fraction	protein (mg)	total act. (units)	sp act. (units/mg)	recovery (%)	x-fold purification
crude extract	18	129	7.2	100	1
IDA–Cu(II)–IMAC	5.2	na	na	na	3.9[b]
Mono-Q	4.2	108	25.3	84	4.2

[a] sp act. is the specific activity determined as described in the Experimental Procedures section; na means that no data are available due to strong inhibition by Cu^{2+}. [b] Theoretical value based on the assumption that 100% purification of fully active XI has been achieved.

Table II: Kinetic Parameters and Heat Stability of D-Xylose Isomerase Purified by IDA–Cu(II)–IMAC[a]

purification method	k_{cat}(xylose) (s^{-1})	K_M(xylose) (mM)	$K_M(Mg^{2+})$ (mM)	$k_D \times 10^{-3}$ (min^{-1})
standard	17.3	4.8	0.08	3.5
IDA–Cu(II)–IMAC	21.0	6.2	0.06	3.5

[a] Steady-state kinetic parameters are derived from fitting the data to the Michaelis–Menten equation (Michaelis & Menten, 1913) using the GraphPad software. k_D is the first-order inactivation rate constant at 84 °C in 50 mM EPPS, pH 7.5, 5.0 mM $MgSO_4$, determined as previously reported (Mrabet et al., 1992).

and most important one elutes with a retention time of 20 min. Figure 6B displays the absorbance spectra for the two peaks and clearly identifies peak II as a protein peak; peak I is bluish, contains no detectable protein, and likely consists of a mixture of imidazole and copper ions. Hence, Mono-Q HPLC further confirms the homogeneity of the XI enzyme recovered from IDA–Cu(II)–IMAC. The protein sample was further dialyzed against 10 mM MES, pH 6.0, after Mono-Q, to remove excess EDTA and salt. Copper determination by atomic absorption spectrometry reveals that residual metal amounts to not more than 0.08 atom/$mol_{tetramer}$.

4. Characterization of XI Purified by IDA–Cu(II)–IMAC, after the Mono-Q Polishing Step. After IDA–Cu(II)–IMAC and Mono-Q, the purified XI displays an enzymatic activity (Table I) comparable to that observed with enzyme purified according to the scheme of Figure 1. The specific activity of the latter is 24 units/mg of protein, which suggests full enzymatic recovery with the IDA–Cu(II)–IMAC/Mono-Q approach. Table I also shows that the overall recovery of enzyme is higher than 80%.

XI enzymes purified using the two different routes were further tested for their kinetic parameters and for their thermostability, with the results indicated in Table II. Clearly, similar values are obtained regardless of the purification protocol used, except that recovery of functional enzyme, as monitored by k_{cat}, appears to be improved with the use of IDA–Cu(II)–IMAC. Given that Cu^{2+} is inhibitory to XI, these data also provide further evidence for the effective elimination of the metal ion from the enzyme by chromatography on Mono-Q in presence of EDTA.

5. Probing the Role of Histidine Residues in the IMAC Recognition Event. Histidine residues have been attributed a dominant role as electron donors in the adsorption process to immobilized metal ions (Sulkowski, 1985, 1989; Hemdan et al., 1989). Histidine residues in XI that are exposed to solvent are listed in Table III. Their accessibility to IDA–Cu(II) was further examined using a spherical surface probe that mimics the tridimensional structure of the Sepharose-coupled metal–chelate affinity ligand around the copper contact region (described below; see Figure 7). Molecular modeling of R–IDA–Cu(II) generates the structure shown in Figure 7B (see also Experimental Procedures section), in which only the metal ligands belonging to IDA have been considered. Completing the coordination about Cu(II), with, e.g., solvent

Table III: Variation with Probe Size of the Static Accessibility of Solvent-Exposed Histidine Residues in D-Xylose Isomerase[a]

probe size	R = 1.4 Å				R = 1.93 Å				decrease in
subunit	A	B	C	D	A	B	C	D	ASA (%)
His-41	73.69	66.26	64.63	70.11	70.12	62.55	60.55	64.86	6.1
His-54	11.64	10.30	8.86	11.07	4.65	4.13	3.50	4.32	60.4
His-96	11.80	10.21	9.85	11.33	4.83	4.12	3.38	5.02	59.8
His-250	40.92	40.49	41.98	40.56	10.53	11.03	10.49	10.41	74.1

[a] The accessible surface areas (Å^2) of histidine residues in wild-type XI were determined using a probe radius of 1.4 Å representing the water molecule or 1.93 Å representing a spherical probe derived from the modeled structure of the *N*-[3-((3′-methoxy-2′-hydroxypropyl)oxy)-2-hydroxypropyl]-IDA–Cu(II) ligand (see Experimental Procedures and Results sections and Figure 7). The 5% cutoff threshold (9.7 Å^2 for histidine) of Miller et al. (1987) was used to distinguish buried from exposed residues. Note that this cutoff value makes His-54 not "accessible" to water molecules only in subunit C. The decrease in ASA observed by increasing the probe size from 1.4 to 1.93 Å is expressed as the absolute percent change averaged over the four subunits.

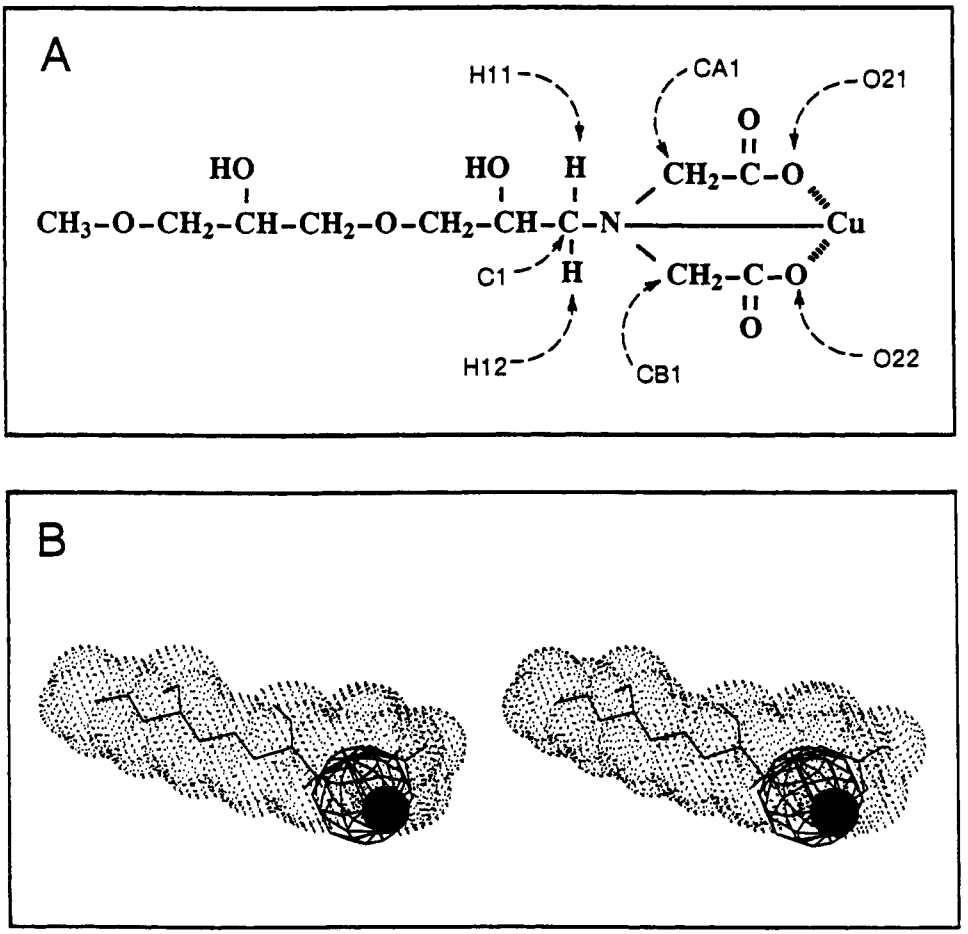

FIGURE 7: Modeled structure of *N*-[3-((3′-methoxy-2′-hydroxypropyl)oxy)-2-hydroxypropyl]-IDA–Cu(II). Panel A shows the chemical structure of R–IDA–Cu(II). Only atoms of interest are labeled. Panel B is a stereo representation of the modeled structure and of the probe sphere used in this study to analyze the accessibility of amino acyl residues of R–IDA–Cu(II). The van der Waals surface of the "desolvated" R–IDA–Cu(II) molecule is shown as a Connolly surface in dots (Connolly, 1983) and was generated by using a solvent probe sphere with radius 0. The 1.93-Å probe sphere is represented by an "open" polyhedron surrounding the copper atom shown as a black sphere. In this side view, both the oxygen and the hydrogen pairs, O21 and O22 and H11 and H12, are being juxtaposed perpendicularly to the plane of the figure so that a plane of the contact surface—represented by atoms Cu, O21, O22, H11, and H12—between R–IDA–Cu(II) and the protein would be horizontal and perpendicular to the figure. For the sake of simplicity, the only nonpolar hydrogens shown in the wire structure are those of the "contact surface", H11 and H12.

molecules, to generate the octahedral structure will obviously lead to an increase in the size of the molecule. The "desolvated" R–IDA–Cu(II) model shown here, however, is a realistic representation of the ligand as it enters in contact with electron donors on the protein. Figure 7B shows that the molecule is slightly kinked at carbon C1 so that a "minimal" contact surface of the ligand to the protein is expected to include the copper atom and its two coordinating oxygens as well as the nearby protruding hydrogens designated H11 and H12 in Figure 7A. On this basis, the probe sphere is centered on the geometric center of the group of atoms that constitute such contact surface. The sphere is then built to also enclose the copper atom and be tangent to its van der Waals surface. Its radius is calculated to be 1.93 Å. In Figure 7B, this spherical probe is represented by the large "open" polyhedron surrounding the copper atom shown as a black sphere. ASA computation with the 1.93-Å-radius sphere indicates that only two histidines at positions 41 and 250 can establish contacts with the probe. Histidine 250 lies in a deep cleft which is located at the interface between protein subunits. This cleft is connected to the external surface of the enzyme and is accessible to water-sized molecules. This is illustrated in Figure 8A which renders the molecular, or Connolly, surface of the protein around this position in subunits A and D,

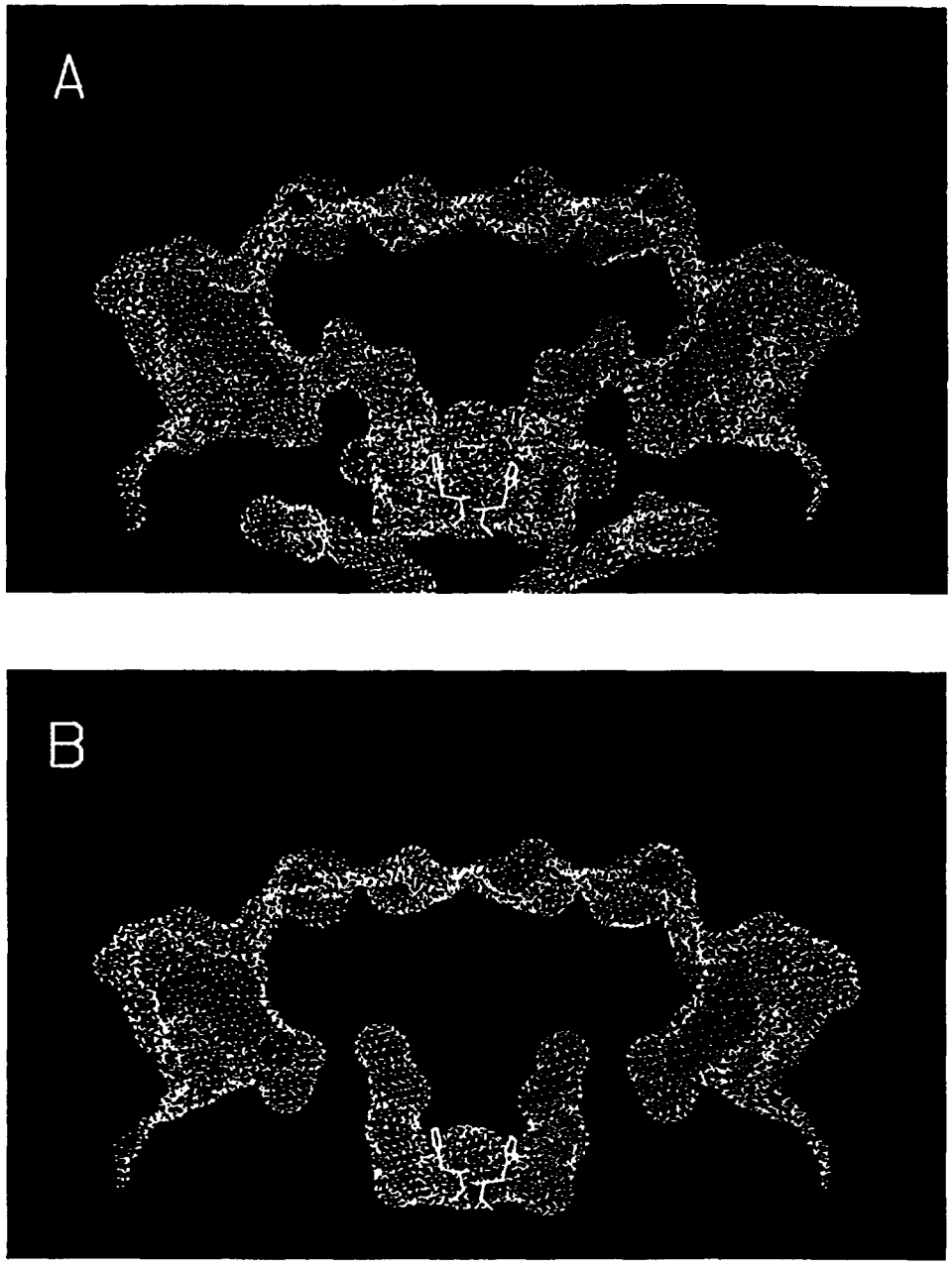

FIGURE 8: Probe-size-dependent variation of the Connolly molecular surface around histidines 250 in subunits A and D of D-xylose isomerase. The molecular surface of D-xylose isomerase is shown in dots (Connolly, 1983) as a cross-section including histidines 250 of subunits A and D. In panel A, a solvent sphere probe of radius 1.4 Å is used, clearly delineating the deep meandering channel which contains histidine 250 and is part of the solvent-accessible external surface of the protein. Increasing the size of the probe radius to 1.93 Å yields the molecular surfaces shown in panel B. Here, histidine 250 is no longer connected to the protein external surface, but instead resides in an "enclosed" cavity that is itself buried within the protein. Only histidines 250 in subunits A and D are shown. The protein cross-section is shown facing the bulk solvent which occupies the top and sides of the figure.

showing how these histidines are related by 2-fold symmetry in the assembled protein tetramer and hence belong to a unique channel that goes through the entire molecule. Note, however, that, regardless of probe size, His 250 accessibility to non-spherical probes might be quite limited due to the convoluted shape of the cleft. Moreover, using the larger probe size of 1.93 Å leads to significant changes in the molecular surface around His 250 (Figure 8B): Histidine 250 is now completely enclosed in a cavity which, although filled with "probe-sized" solvent molecules, no longer has access to the external surroundings. On this basis, the implication of this residue in IMAC is deemed dubious (see Discussion section below).

A. missouriensis XI contains five tryptophan residues per subunit, but all are shielded from interaction with chromatographic surfaces. Furthermore, the protein is totally devoid of cysteine residues. As described above, each XI subunit contains two metal binding sites, but these are found deeply buried in a 20-Å-deep cleft leading to the catalytic center of the enzyme.

Taken altogether, these data suggest that histidine 41 constitutes the most plausible candidate for interacting with immobilized metal–chelates.

The respective role of surface histidine residues 41 and 96 in XI adsorption to IDA–Cu(II) was assessed by site-directed mutagenesis. Mutants H41K and H96K were engineered and expressed in *E. coli* as soluble proteins. The basis for studying the role of position 96 is that, although this residue is not accessible to the "IDA–Cu(II)" probe used in this study (Table III), its location on the external surface, at the interface between protein and solvent, suggests that very minor changes

Table IV: Enzymatic Properties and Heat Stability of Surface Histidine Mutants of D-Xylose Isomerase[a]

mutant	sp act. (units/mg)	K_M(xylose) (mM)	$K_M(Mg^{2+})$ (mM)	$k_D \times 10^{-3}$ (min^{-1})
H41K	26	4.9	0.17	7
H96K	25	nd	0.16	37

[a] sp act. is the specific activity determined as previously described (Mrabet et al., 1992). Steady-state kinetic parameters were determined by fitting the data to the Michaelis–Menten equation (Michaelis & Menten, 1913) using the GraphPad software. k_D is the first-order inactivation rate constant at 84 °C in 50 mM EPPS, pH 7.5, 5.0 mM $MgSO_4$, determined as previously described (Mrabet et al., 1992). nd indicates not determined.

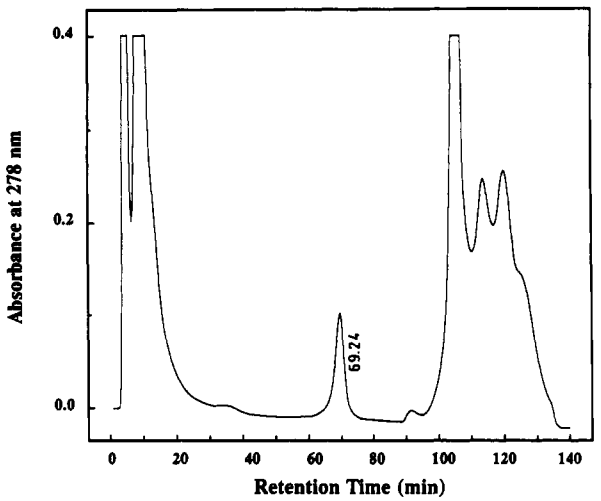

FIGURE 9: IDA–Cu(II)–IMAC of the H96K mutant of D-xylose isomerase. The sample is an aliquot of total cell lysate (0.5 mL; ~19 mg/mL) from *E. coli* producing the XI mutant, H96K. Solvents and gradient program are those described in the legend to Figure 5.

in conformation that can be caused by solvents or interactions with chromatographic surface may expose this residue. This principle does not apply to histidine 54 which is located within the active site at the bottom of a 20-Å-deep cleft and is therefore not likely to be engaged in IMAC. The expression level of H41K was similar to that of wild-type enzyme, while that of H96K was reduced about 3-fold. Both mutants could be purified following the standard protocol in Figure 1: Remarkably, under these conditions, their chromatographic behavior is found to be *indistinguishable* from that of wild type. Furthermore, both display catalytic properties similar to those of the wild type (Table IV). The thermostability of these mutants was also tested (Table IV). At 84 °C, H41K decays about twice as fast as wild type, while H96K is more unstable with a 10-fold reduction in half-life. Molecular modeling (not shown) suggests that these substitutions can be accommodated within the three-dimensional structure of wild-type XI with no steric clash or electrostatic incompatibility, particularly for H41K as this position is fully surrounded by solvent on the surface of the protein. Taken together, these data suggest that at least mutant H41K has an overall conformation similar to that of the wild-type enzyme. Therefore, a difference in behavior in IDA–Cu(II)–IMAC should be interpreted to reflect the effect of removing the electron-donor character ascribed to histidine residues.

IDA–Cu(II)–IMAC of mutant H96K gives an elution profile identical to that of the wild-type protein (Figure 9). This finding therefore eliminates the contribution of histidine 96 to the retention of XI onto the IDA–Cu(II) matrix. In contrast, substituting lysine for histidine at position 41 has profound consequences on the chromatographic behavior of

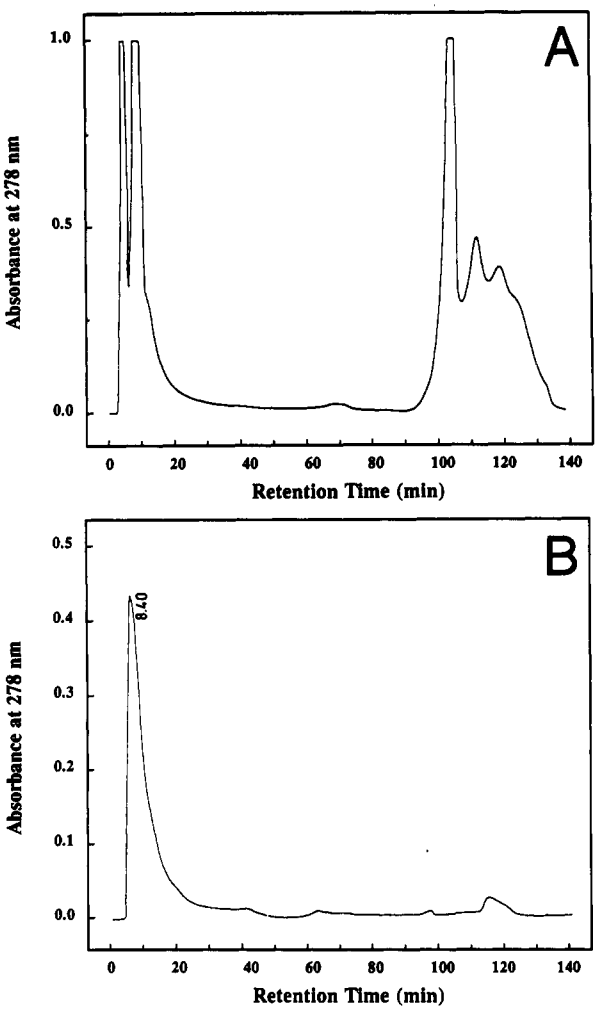

FIGURE 10: IDA–Cu(II)–IMAC of the H41K mutant of D-xylose isomerase. Panel A shows the chromatography on IDA–Cu(II)–IMAC of an aliquot (0.5 mL; ~22 mg/mL) from total cell lysate from *E. coli* producing the XI mutant, H41K. Panel B is the IMA chromatogram of mutant H41K (0.5 mL; 5 mg/mL) purified by the traditional procedure of Figure 1. Solvents and gradient program are those described in the legend to Figure 5.

the variant: IDA–Cu(II)–IMAC of the total cell lysate shows that this mutation leads to complete disappearance of the absorbance peak with a retention time of 69 min (Figure 10A), while the "background" absorbance peaks remain unaltered. SDS–PAGE of the chromatographic fractions (not shown) as well as IDA–Cu(II)–IMAC of the H41K mutant that had been previously purified according to the traditional protocol of Figure 1 further establishes that adsorption to IDA–Cu(II) is totally abolished as the protein elutes in the flow-through, unretarded (Figure 10B).

Discussion

Protein purification has been a challenging issue because separation schemes must ideally take into consideration several objectives: (i) obtain the required level of purity, (ii) recover sufficient amounts of purified material, (iii) preserve biological activity, and (iv) be cost-effective.

Pseudoaffinity purification methods such as IMAC show considerable potentialities to fulfill these requirements [see, e.g., Arnold (1991) for a review]. Our understanding of the mechanisms which govern selectivity in immobilized metal recognition by proteins is, however, limited and for the most part phenomenological. This has hampered progress in protocol design for the purification of "natural" proteins. Most efforts have, instead, been directed at incorporating affinity

tags to proteins by recombinant DNA methods.

The work described here yet provides evidence that refined modulation of environmental factors such as pH and ionic strength can lead to remarkable selectivity enhancement in the interaction of a protein, xylose isomerase, with IDA–Cu(II).

1. Requirements for Protein Adsorption and Desorption in IMAC. Binding to immobilized metal–chelates by formation of a coordination bond requires that one or more electron-donating groups residing on the surface of the protein be at least partially unprotonated. As a consequence, protein adsorption to IDA–Me(II) is influenced by pH (Sulkowski, 1987) and by the presence in the surrounding solvent of effector molecules also capable of interacting with the metal–chelate. Furthermore, several chromatographic modes (IMAC, hydrophobic interaction, and cation exchange) can operate simultaneously in IMAC (Figueroa et al., 1986).

Thus, by and large, experimental variables such as pH, ionic strength, salt type and concentration, temperature, the nature of the metal ion used, and the presence and nature of effector molecules can all contribute to affect the ligand–ligate affinity interaction in IMAC (Gutman, 1978; Hansson & Kågedal, 1981; Porath & Olin, 1983; Sulkowski, 1987; N. T. Mrabet, unpublished results).[7]

Elution of bound protein from the metal–chelate sorbent results from the breakage of the coordination bond(s) formed between ligand and ligate. To achieve heterolytic cleavage will clearly depend upon the strength of the coordination bond(s) established at the time of adsorption [see, e.g., the "bond-length variation rules" in Gutmann (1978)].

Different approaches have been successfully utilized to convey protein elution from metal–chelate matrices. These have included (i) reducing the pH, i.e., protonating the electron-donating group on the protein; (ii) displacing the bound protein with a competitive ligand such as imidazole; or (iii) stripping the matrix-bound metal ions—and thus, all components attached to them—with a strong chelator such as EDTA. Yet, the combination of pH, salt, and imidazole effects by means of a ternary gradient had not been exploited before the present study.

2. Optimizing IMA Selectivity. Important aspects which contribute to the differential retention behavior of proteins onto IDA–Cu(II) have been reviewed recently (Sulkowski, 1987) and include (i) the accessibility and number of the electron-donating group(s) present in the protein, (ii) their microenvironment, which in particular defines the pK_a and hence the electron-donating properties of the residue(s) involved, and (iii) the presence or absence of clusters of metal ligands which are known to enhance metal binding affinity by chelate effect.

Here, a clear emphasis has been further put on the structural and physical–chemical properties of xylose isomerase in order to establish rational approaches to selectivity engineering for purification by IDA–Cu(II)–IMAC.

In agreement with other investigators (Sulkowski et al., 1982; Porath & Olin, 1983; Muszynska et al., 1986), I first show that protein binding to IDA–Cu(II) can occur under slightly acidic conditions: XI is effectively adsorbed to Cu(II)-Chelating Sepharose at pH 6.0 in the presence of 0.5 M NaCl. The presence of salt in the equilibration solvent facilitates the close contact of the electron-donating residue(s) with the metal (Purcell & Klotz, 1977; Wu et al., 1986) and also provides for the screening of nonspecific electrostatic interactions: XI binds to Cu(II)–Chelating Sepharose *only* in the presence of high salt, a behavior which is likely explained by the need to quench the electrostatic repulsion between this highly negatively-charged protein and an affinity sorbent that is itself predominantly negatively charged (Sulkowski, 1987). At pH 6.0, half of the histidyl side chains ($pK_a \simeq 6$) present on the surface of the protein are uncharged and, hence, can establish a coordination bond to the immobilized copper ion. Further partitioning of the unprotonated species onto the metal–chelate sorbent is expected to shift the equilibrium toward unprotonated imidazole and thereby ensures that all the xylose isomerase is ultimately adsorbed.

The knowledge that the overall charge of IDA–Cu(II) is negative has further led to the strategy involving the reduction of both pH and ionic strength to enhance the electrostatic repulsion between XI and IDA–Cu(II) and to thereby facilitate desorption of the bound enzyme. The chromatogram in Figure 2 shows that XI still displays effective binding affinity to IDA–Cu(II) near pH 5 since elution is obtained only after percolating 4.4 mL of the pH 5.0 solvent mixture. The occurrence of such an affinity is clearly illustrated by the observation that minor adjustments in the composition of the solvent mixtures during column equilibration and the first period of descending pH gradient lead to further delaying XI desorption so as to require the presence of 1–2 mM imidazole at pH $\simeq$ 5.1. Thus, selectivity is achieved by a judicious combination of solvent parameters involving the modulation of electrostatic versus metal-coordination interactions.

Xylose isomerase recovered from IDA–Cu(II)–IMAC is strongly inhibited due to the presence of contaminating copper ions. Reactivation of the enzyme is however readily accomplished by chromatography on Mono-Q in presence of EDTA, a polishing step which yields a protein similar in every aspect to that obtained by standard purification. Yet, preliminary data suggest that full recovery of biological activity is optimized with IMAC. Such finding is expected from the elimination of several (five total) steps in the traditional purification protocol, particularly those which may trigger protein denaturation.

3. Implication of Histidine 41 in the IMA Recognition Event. A predominant role for surface histidines has been set forth to interpret the chromatographic behavior of natural proteins and peptides in IDA–Cu(II)–, IDA–Ni(II)–, and IDA–Zn(II)–IMAC (Sulkowski, 1987, 1989; Hemdan et al., 1989; Yip et al., 1989; Arnold, 1991), but the *specific* contribution of this residue was not demonstrated before the present study.

It is shown here that site-directed mutagenesis in combination with X-ray structure analysis and molecular modeling does offer an effective means to tackle this issue. Investigations have been conducted into the sites in XI that could interact with immobilized IDA-Cu(II). The accessibility of amino acid residues with electron donor character, particularly histidines, was analyzed using a spherical probe whose size was determined on the basis of a model structure of the IDA–Cu(II) ligand that is attached to Sepharose and is designated here as R–IDA–Cu(II). A number of comments must be made in this respect. First, the model of R–IDA–Cu(II) described in this study yields the smallest probe size: (i) changing the metal-coordination geometry in IDA–Cu(II), e.g., to square

[7] In the course of this study, it was observed that XI adsorption onto IDA–Cu(II) is substantially stronger in the presence of K_2SO_4 than NaCl, and also at pH 8 rather than at pH 6; as an example, when XI is bound to Cu(II)–Chelating Sepharose Fast Flow at pH 7.0 in the presence of 0.25 M K_2SO_4, protein desorption does not take place when the pH is reduced to 5, and it only occurs after the imidazole concentration has reached 25 mM; as shown in Figure 2, substitution of NaCl for K_2SO_4 at equinormal concentration, under conditions that are otherwise identical, leads to enzyme elution at pH 5.

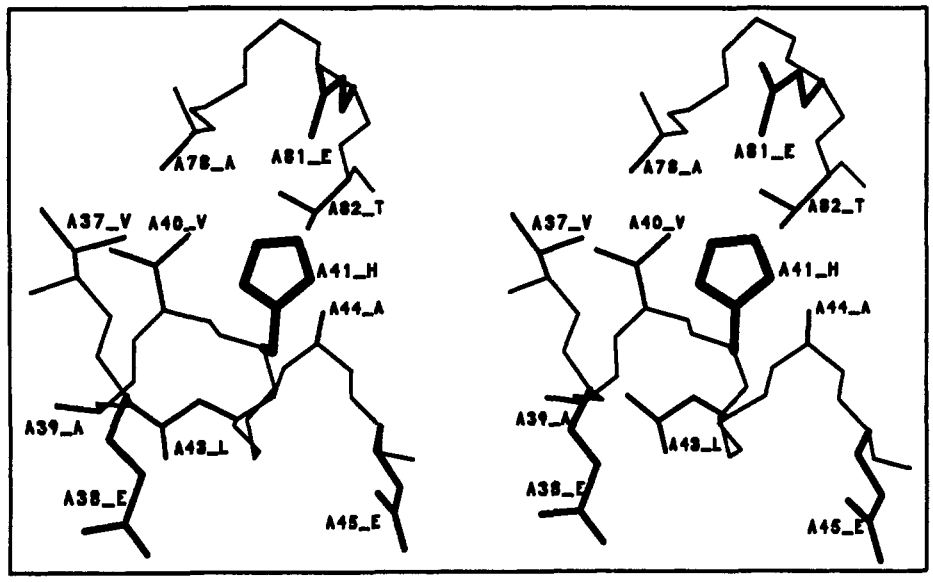

FIGURE 11: Structure of wild-type D-xylose isomerase around histidine 41. This view shows histidine 41 of subunit A facing the solvent. Only side chains of interest are represented. His 41 and surrounding glutamates are shown in bold. For the sake of simplicity, hydrogen atoms and main-chain oxygens have been omitted.

planar, indeed increases the radius of the probe up to a value of 3.5 Å (N. T. Mrabet, unpublished data); (ii) computation of the probe radius did not take into account other, non-IDA, coordination ligands (e.g., solvent molecules) which would contribute to an *increase* in the size of the probe, assuming that these are easily displaceable and therefore not likely to contribute in a significant fashion to controlling IDA–Cu(II) accessibility. Second, it should be emphasized that increasing the size of the probe should not significantly affect, if at all, the accessibility of protruding residues which are most effective at recognizing large ligands. This is illustrated in Table III, where the change in ASA for His 41 is only ~6%, whereas that of His 250 is reduced nearly 4-fold. ASA computation *alone* indicates that His 250 remains "accessible" (~10 Å^2) to the IDA–Cu(II) probe. However, this residue is in fact found in a cavity filled with "solvent" but is also totally surrounded by the protein. This cavity is shown to open up to the "outside world" by reducing the probe size from 1.93 to 1.4 Å (see Figure 8). These observations have two fundamental implications in the understanding of protein–ligand interactions: First, the dimensions of the spherical probe used to determine residue accessibility must be calculated starting from an appropriate structure of the ligand of interest. Second, as illustrated in Figure 8B, surface areas alone cannot provide unequivocal conclusions regarding residue accessiblity. Finally, only static accessibilities are calculated, and therefore one should not exclude a priori the contribution of some "buried" residues. This explains why "surface" mutant H96K was tested. The participation of His 250 was not investigated further, given that this residue is located in a deep cleft within the interface between subunits in a very stable protein which remains undissociated even in 10 M urea (Mrabet et al., 1992; N. T. Mrabet, manuscript in preparation).

Histidine 41 was identified as the most likely candidate to interact with immobilized copper–chelate. Replacement with lysine yields a mutant enzyme with physical–chemical properties similar to those of wild type. Yet, this amino acid replacement suppresses XI retention onto the IDA–Cu(II) column. If electron-donor residues other than His 41 had been independently involved in binding IDA–Cu(II), it is expected that some retardation of the protein onto the metal–chelate matrix would have occurred, but this is not observed. Maintenance of an otherwise constant background of the protein molecular surface in the H41K mutant, which is also suggested by molecular modeling studies, hence provides the unequivocal demonstration that histidine 41 is the predominant ligand implicated in IDA–Cu(II) adsorption. Figure 11 shows the structure of D-xylose isomerase around residue 41 facing the solvent. This position resides at a protein/solvent interface where the protein background is mostly nonpolar. A few polar residues, including histidine 41, point outward. These include glutamates 38, 45, and 81 which all surround His 41 and, in conjunction with this residue, may possibly participate in metal coordination.

In conclusion, the present study shows that IDA–Cu(II)–IMAC is amenable to rational optimization such that *A. missouriensis* D-xylose isomerase can be purified in a single chromatographic step starting from crude cell lysate. This pseudoaffinity technique is convenient and fast and it permits easy scale-up.[8] Chelating Sepharose Fast Flow provides chromatographic separation with high-performance resolution. IMAC is a mild purification procedure which avoids often unrecognized protein denaturation events likely to be encountered in traditional multistep purification protocols. Finally, elucidation of the role of histidine 41 as a predominant ligand to the metal–chelate sorbent further suggests that IMAC can be operated to provide for the single-step purification of other proteins that contain at least one solvent-exposed residue with electron-donating character. Alternatively, one could envision further stratagems that bear on introducing histidine residues at defined sites in recombinant proteins, in particular by means of semiconservative amino acid replacements where histidine is substituted for asparagine or glutamine.

ACKNOWLEDGMENTS

I thank Dr. Partrick Stanssens and Marijke Beyaert for providing the *E. coli* clones expressing recombinant wild-type and mutant D-xylose isomerase enzymes described in this study, Dr. Marc Lauwereys and Adri Van Vliet for the purification of enzymes according to the traditional protocol, Drs. Philippe Alard, Ignace Lasters, Michel Bardiaux, and Philippe

[8] N. T. Mrabet and A. Van Vliet, unpublished results. A total of 250 mg of protein could be loaded onto a (2 × 20 cm) Cu(II)–Chelating Sepharose Fast Flow column to allow recovery of 50 mg of pure XI.

Delhaise for help and advice with the BRUGEL package, and Dr. Michel Honig of the Research Institute of the Belgian Ministry of Agriculture for metal determination. The expert assistance of Roland Gordon-Beresford in molecular modeling is gratefully acknowledged. I am deeply thankful to Dr. Shoshana Wodak for continuous interest and support during the course of this study, and to Dr. Moshe M. Werber for insightful comments on the manuscript. I wish to express my gratitude to Dr. Eugene Sulkowski for invaluable advice and discussions and for reviewing an early version of the manuscript.

REFERENCES

Alard, P. (1991) Ph.D. Dissertation, Université Libre de Bruxelles, Faculté des Sciences, Brussels, Belgium.

Alber, T., Dao-pin, S., Nye, J. A., Muchmore, D. C., & Matthews, B. W. (1987) *Biochemistry 26*, 3754–3758.

Arnold, F. H. (1991) *Bio/Technology 9*, 151–156.

Belew, M., Yip, T.-T., Andersson, L., & Ehrnström, R. (1987) *Anal. Biochem. 164*, 457–465.

Bradford, M. M. (1976) *Anal. Biochem. 72*, 248–254.

Carrell, H. L., Glusker, J. P., Burger, V., Tritsch, D., & Bieleman, J.-F. (1989) *Proc. Natl. Acad. Sci. U.S.A. 86*, 4440–4444.

Colson, C., Clocer, S. W., Sijmonds, N., & Stacey, K. (1965) *Genetics 52*, 1043–1050.

Connolly, M. L. (1983) *Science 221*, 709–713.

Delhaise, P., Bardiaux, M., & Wodak, S. J. (1984) *J. Mol. Graphics 2*, 103–106.

Figueroa, A., Corradini, C., Feibush, B., & Karger, B. L. (1986) *J. Chromatogr. 371*, 335–352.

Fletcher, R., & Reeves, C. M. (1964) *Comput. J. 6*, 163–168.

Good, N. E., Winget, G. W., Winter, W., Connolly, T. N., Izawa, S., & Singh, R. M. M. (1966) *Biochemistry 5*, 467.

Grady, J. K., Chasteen, N. D., & Harris, D. C. (1988) *Anal. Biochem. 173*, 111–115.

Gutmann, V. (1978) in *The Donor–Acceptor Approach to Molecular Interactions*, Plenum Press, New York.

Hansson, H., & Kågedal, L. (1981) *J. Chromatogr. 215*, 333–339.

Hegetschweiler, K., & Saltman, P. (1986) *Inorg. Chem. 25*, 107–109.

Hemdan, E. S., Zhao, Y., Sulkowski, E., & Porath, J. (1989) *Proc. Natl. Acad. Sci. U.S.A. 86*, 1811–1815.

Howard-Flanders, P., Boyce, R. P., & Theriot, L. (1966) *Genetics 53*, 1119–1136.

Hutchens, T. W., & Yip, T.-T. (1990) *J. Chromatogr. 500*, 531–542.

Hutchens, T. W., Yip, T.-T., & Porath, J. (1988) *Anal. Biochem. 170*, 168–182.

Kasumi, T., Hayashi, K., & Tsumura, N. (1982) *Agric. Biol. Chem. 46*, 31–39.

Kersters-Hilderson, H., Callens, M., Van Opstal, O., Vangrysperre, W., & De Bruyne, C. K. (1987) *Enzyme Microb. Technol. 9*, 145–148.

Lee, B., & Richards, F. M. (1971) *J. Mol. Biol. 55*, 379–400.

Maniatis, T., Fritsch, E. F., & Sambrook, J. (1982) *Molecular Cloning: A Laboratory Manual*, Cold Spring Harbor Laboratory, Cold Spring Harbor, NY.

Miller, S., Janin, J., Lesk, A. M., & Chothia, S. (1987) *J. Mol. Biol. 196*, 641–656.

Mrabet, N. T., Van den Broeck, A., Van den Brande, I., Stanssens, P., Laroche, Y., Lambeir, A. M., Matthyssens, G., Jenkins, J., Chiadmi, M., van Tilbeurgh, H., Rey, F., Janin, J., Quax, W. J., Lasters, I., De Maeyer, M., & Wodak, S. J. (1992) *Biochemistry 31*, 2239–2253.

Muszynska, G., Andersson, L., & Porath, J. (1986) *Biochemistry 25*, 6850–6853.

Porath, J., & Olin, B. (1983) *Biochemistry 22*, 1621–1630.

Porath, J., Carlsson, J., Olsson, I., & Belfrage, G. (1975) *Nature 258*, 598–599.

Purcell, K. F., & Klotz, J. C. (1977) *Inorganic Chemistry*, Saunders, Philadelphia, PA.

Regnier, F. (1987) *Science 238*, 319–323.

Rey, F., Jenkins, J., Janin, J., Lasters, I., Alard, P., Claessens, M., Matthyssens, G., & Wodak, S. J. (1988) *Proteins: Struct., Funct., Genet. 4*, 165–172.

Sanger, F., Nicklen, S., & Coulson, A. R. (1987) *Proc. Natl. Acad. Sci. U.S.A. 74*, 5463–5467.

Shannon, R. D. (1976) *Acta Crystallogr. A32*, 751.

Stanssens, P., Opsomer, C., McKeown, Y. M., Kramer, W., Zabeau, M., & Fritz, H. J. (1989) *Nucleic Acids Res. 17*, 4441–4454.

Sulkowski, E. (1985) *Trends Biotechnol. 3*, 1–7.

Sulkowski, E. (1987) in *UCLA Symposia on Molecular and Cellular Biology, New Series* (Burgess, R., Ed.) Vol. 68, pp 149–162, Liss, New York.

Sulkowski, E. (1989) *BioEssays 10*, 170–175.

Sulkowski, E., Vastola, K., Oleszek, D., & Von Muenchhausen, W. (1982) in *Affinity Chromatography and Related Techniques* (Gribnau, T. J. C., Visser, J., & Nivard, R. J. F., Eds.) pp 313–322, Elsevier, Amsterdam, The Netherlands.

Sundberg, R. J., & Martin, R. B. (1974) *Chem. Rev. 74*, 471–517.

Wu, S. L., Figueroa, A., & Karger, B. L. (1986) *J. Chromatogr. 371*, 3–8.

Yip, T.-T., Nakagawa, Y., & Porath, J. (1989) *Anal. Biochem. 183*, 159–171.